EUKARYOTIC CELL, Dec. 2006, p. 2174–2183 Vol. 5, No. 12
1535-9778/06/$08.00+0 doi:10.1128/EC.00163-06

Targeted Deletion of *MIC5* Enhances Trimming Proteolysis of *Toxoplasma* Invasion Proteins▽

Susannah D. Brydges,[1]† Xing Wang Zhou,[1]‡ My-Hang Huynh,[1]§ Jill M. Harper,[1]¶ Jeffrey Mital,[2] Koku D. Z. Adjogble,[3] Walter Däubener,[3] Gary E. Ward,[2] and Vern B. Carruthers[1]*

W. Harry Feinstone Department of Molecular Microbiology and Immunology, Johns Hopkins Bloomberg School of Public Health, Baltimore, Maryland 21205[1]; Department of Microbiology and Molecular Genetics, University of Vermont, Burlington, Vermont 05405[2]; and Institute for Medical Microbiology and Hospital Hygiene, Universitaetsstr. 1, D-40225 Düsseldorf, Germany[3]

Received 3 June 2006/Accepted 1 September 2006

Limited proteolysis of proteins transiently expressed on the surface of the opportunistic pathogen *Toxoplasma gondii* accompanies cell invasion and facilitates parasite migration across cell barriers during infection. However, little is known about what factors influence this specialized proteolysis or how these proteolytic events are regulated. Here we show that genetic ablation of the micronemal protein MIC5 enhances the normal proteolytic processing of several micronemal proteins secreted by *Toxoplasma* tachyzoites. Restoring MIC5 expression by genetic complementation reversed this phenotype, as did treatment with the protease inhibitor ALLN, which was previously shown to block the activity of a hypothetical parasite surface protease called MPP2. We show that, despite its lack of obvious membrane association signals, MIC5 occupies the parasite surface during invasion in the vicinity of the proteins affected by enhanced processing. Proteolysis of other secretory proteins, including GRA1, was also enhanced in MIC5 knockout parasites, indicating that the phenotype is not strictly limited to proteins derived from micronemes. Together, our findings suggest that MIC5 either directly regulates MPP2 activity or it influences MPP2's ability to access substrate cleavage sites on the parasite surface.

Members of the phylum *Apicomplexa* are obligate intracellular parasites that replicate in a variety of cell types. Some, including the human pathogens *Plasmodium* and *Babesia*, replicate primarily in the bloodstream, whereas others such as *Cryptosporidium*, a cause of chronic gastritis among the immune-compromised, and *Eimeria*, an agricultural parasite, replicate in the intestinal epithelium. Only parasites in the isosporoid coccidian clade, which includes *Toxoplasma gondii*, the causative agent of toxoplasmosis, replicate in deep tissues (2). Thus, it can be expected that each clade has its own complement of proteins facilitating survival in a specific habitat, along with conserved proteins that play fundamental roles in events common to all apicomplexans.

Many invasion studies have been performed in *T. gondii*, as it is more amenable to in vitro manipulation than other members of the *Apicomplexa*. Upon contact with a host cell, *T. gondii* tachyzoites discharge the contents of apically localized microneme (MIC) organelles (13). MIC adhesive proteins contribute to binding host cell receptors, and blocking micronemal secretion dramatically reduces invasion (9). These proteins, which often cluster into multiunit complexes, are transiently deployed to the apical surface during apical attachment and invasion. Transmembrane (TM) MIC proteins, such as MIC2, MIC6, and MIC8, are thought to act as bridging molecules that connect host receptors with the parasite's motility apparatus, the glideosome (37). By translocating MIC-receptor complexes backwards toward the posterior end, the parasite "pulls" itself into the target cell, invaginating the host plasma membrane to form the nascent parasitophorous vacuole (PV). As they treadmill posteriorly, MIC proteins are processed by hypothetical surface proteases known as MPP1, MPP2, and MPP3, which have been characterized based on their cleavage site specificity and susceptibility to inhibitors (5, 11, 36, 43). MPP1 is an intramembrane protease of the rhomboid family (7, 11, 19, 36) that sheds MIC complexes from the parasite surface during the final seconds of invasion. Although MPP2 and MPP3 are known to trim MIC substrates on the parasite surface, the identity of these proteases and functional consequences of their processing remain unknown.

Here we use genetic ablation and proteomic profiling to show that a small MIC protein called MIC5 that is conserved among isosporoid coccidian parasites influences surface proteolysis by MPP2 and possibly MPP3. Our findings indicate that MIC5 either directly regulates the activity of these proteases or influences the proteolytic susceptibility of other MIC substrates.

MATERIALS AND METHODS

Sequence database searches. The MIC5 amino acid sequence (GenBank accession no. CAA70921) was used to search the following databases: NCBI non-

* Corresponding author. Present address: Department of Microbiology and Immunology, University of Michigan School of Medicine, 1150 W. Medical Center Drive, Ann Arbor, MI 48109. Phone: (734) 763-2081. Fax: (734) 764-3562. E-mail: vcarruth@jhsph.edu.
† Present address: Genetics and Genomics Branch, National Institute of Arthritis and Musculoskeletal and Skin Diseases, Bethesda, MD 20892.
‡ Present address: Department of Biochemistry and Molecular Biology, University of Maryland School of Medicine, Baltimore, MD 21201.
§ Present address: Department of Microbiology and Immunology, University of Michigan School of Medicine, Ann Arbor, MI 48109.
¶ Present address: Laboratory of Clinical Investigation, Gerontology Research Center, Baltimore, MD 21224.
▽ Published ahead of print on 15 September 2006.

redundant, the NCBI expressed sequence tag, the *Eimeria* genome (http://apidb.org/apidb2.0/index.jsp), the *Cryptosporidium* genome (http://apidb.org/apidb2.0/index.jsp), the *Plasmodium* genome (http://www.plasmodb.org/), and apicomplexan expressed sequence tag genome (http://apidb.org/apidb2.0/index.jsp). BlastP or TBLASTN were used as appropriate. Hits with expect values of $<1 \times 10^{-5}$ were considered significant matches.

Plasmid constructs. pMINI*HXGPRT5′3′MIC5* was generated by inserting *MIC5* 5′ and 3′ flanking sequences upstream and downstream, respectively, of dihydrofolate reductase sequences in the plasmid pMINI*HXGPRT* (18). The 1,557-bp 5′ *MIC5* flanking sequence was PCR amplified from genomic DNA using primers *MIC5*.-1557.KpnI.f (ACGTGGTACCACGCACAGGTGTTTCATTTC) and *MIC5*.-1.HindIII.r (ACGTAAGCTTACAGCCTCAAACTCTTC) (restriction site sequences used to clone into pMINI*HXGPRT* are underlined). The 3′ flank was amplified from construct pSH4A containing the MIC5 genomic locus with primers *MIC5*.3886.SpeI.f (GATCACTAGTCAGGCGACGGTGTGAGG) and *MIC5*.6447.NotI.r (GACTGCGGCCGCTCATGGAACAAACGCACAGAG) using the Expand long template PCR system (Roche) according to the manufacturer's instructions. Both flanking regions were subcloned into the pGEM-T vector (Promega) according to the manufacturer's instructions. Positive bacterial clones were selected by restricting DNA with KpnI and HindIII (5′ flank) and SpeI and NotI (3′ flank). Inserts were then directionally ligated into pMINI*HXGPRT* cut with the same enzymes, dephosphorylated, and gel purified. *MIC5* complementation construct p*MIC5* was prepared as follows. A 5.2-kb region of the genomic *MIC5* locus, including approximately 2.4 kb of 5′ flanking sequence, the complete *MIC5* open reading frame, and 0.5 kb of 3′ flanking sequence, was PCR amplified from *T. gondii* genomic DNA using primers *MIC5*.-2421.f (TGTCGAGATCAAAGCATC) and *MIC5*.1317.r (GTCACCTCTTTAATTGAC). PCR products of the correct size were cloned into pGEM-T. All plasmids were verified by restriction analysis. Preparative scale purifications were made using QIAGEN MAXI preps according to the manufacturer's instructions.

Parasites, transfection, and selection. All parasites were maintained in primary human foreskin fibroblasts (HFF) grown in Dulbecco's modified Eagle's medium (DMEM; Biowhittaker), supplemented with 10% fetal bovine serum (FBS; Sigma), 10 mM HEPES, 2 mM glutamine, and 50 μg ml^{-1} penicillin/streptomycin (Cellgro). Δ*HX* parasites deficient in hypoxanthine-xanthine-guanine phospho-ribosyl transferase (HXGPRTase), which are equivalent to *RHhxgprt*$^-$ (18), were purified by membrane filtration, washed, and resuspended in sterile Cytomix buffer (120 mM KCl, 0.15 mM $CaCl_2$, 10 mM K_2HPO_4/KH_2PO_4, pH 7.6, 25 mM HEPES, 2 mM EDTA, 5 mM $MgCl_2$, pH 7.6). Δ*HX* parasites (1.7×10^7) were electroporated with 5, 10, 15, 25, 50, 75, or 100 μg NotI-linearized pMINI*HXGPRT5′3′MIC5* with a Bio-Rad GenePulsar II (settings, 1.5 kV, 25 μF, no resistance). Following overnight growth in the absence of drug, HXGPRT$^+$ parasites were selected with 25 μg ml^{-1} mycophenolic acid (Sigma) and 50 μg ml^{-1} xanthine (Sigma) for one passage before cloning by limiting dilution under drug selection. Surviving clones were screened for the presence of MIC5 as follows: clonal wells were inoculated into chamber slides (Nunc) of HFF and allowed to grow for 48 h before fixation and immunofluorescence localization as described previously (27) using mouse anti-H4 (MIC5) (29) or rat anti-MIC5, diluted 1:500 and 1:250, respectively. Cells were also stained with antibodies to M2AP as a positive control for microneme staining. Clones negative by immunofluorescence were confirmed negative for MIC5 expression by immunoblotting parasite lysates prepared as described below. Three independent clones: Δ*MIC5*-1, -2, and -3 were genetically complemented by cotransfection with 50 μg supercoiled p*MIC5* and 10 μg p*CAT* (equivalent to p*TUB5CATSag1*; D. Soldati, University of Geneva). Drug-resistant populations were selected with 20 μM chloramphenicol for approximately 2 weeks and were then cloned by limiting dilution as described above. One MIC5$^+$ CAT$^+$ clone, identified by immunofluorescence, generated from each of Δ*MIC5*-1 and Δ*MIC5*-2, was expanded and examined for proper secretion kinetics of MIC5. One MIC5$^-$ CAT$^+$ clone per Δ*MIC5* clone was also expanded. In all further assays, RH parasites were used as a wild-type control strain for comparison. (Although Δ*MIC5* parasites were isolated directly from Δ*HX*, Δ*HX* parasites were not used as they showed inconsistent growth and invasion characteristics, making comparisons difficult.)

Southern blotting. Southern blots were performed essentially as described previously (25), with the following modifications. The MIC5 probe was amplified from a *T. gondii* cDNA library with primers MIC5.45.f (GCTGGTGTGGGTTCTTGATGTAGT) and MIC5.379.r (CCGGGATGTTCTGCCTGTC). Genomic DNA was digested with EcoRV and EcoRI and SnaBI and BclI, respectively. The probe does not contain sites for any of these enzymes.

Antibodies. Antibodies used for immunofluorescence and immunoblotting include the following: monoclonal antibody (MAb) 4F8E12 anti-MIC1 (Jean-François Dubremetz, Montpellier University, France), MAb 6D10 anti-MIC2 (41), MAb T42F3 anti-MIC3 (1), rabbit anti-MIC4 (5), MAb 5B1 anti-MIC4 (12), mouse anti-H4 (29), rat anti-MIC5, rabbit anti-MIC5, rabbit anti-MIC6 N terminus, rabbit anti-MIC6 C terminus, rabbit anti-MIC8 N terminus, rabbit anti-MIC8 C terminus (32), rabbit anti-MIC10 (25), MAb B3.90 anti-AMA1 (17), rabbit anti-M2AP, affinity-purified rat anti-M2AP (39), rabbit anti-PfSUB1 (4), rabbit anti-TgSUB1 (33), MAb G11-9 anti-SAG1 (Argene Biosoft), rabbit anti-SAG1 (L. Kasper, Dartmouth University), rabbit anti-ROP2 (3), MAb Tg17-43 anti-GRA1 (14), MAb 4G1.AH11 anti-GRA4 (31), and rabbit anti-actin (16).

Immunolocalization experiments. Indirect immunofluorescence assays were performed on intracellular parasites as described previously (27). To examine protein localization during invasion, parasites were syringed, filtered, washed, and concentrated in room temperature "Endo" buffer (a potassium-rich solution that arrests parasite motility) (20) before being applied to HFF grown overnight on 8-well chamber slides for 20 min at 37°C. The Endo buffer was replaced with 37°C invasion medium (DMEM supplemented with 20 mM HEPES and 3% fetal bovine serum), and parasites were allowed to invade for 1 min at 37°C before fixation as described previously (27). To selectively permeabilize the host cell plasma membrane and parasitophorous vacuole, but not the parasite plasma membrane, fixed slides were incubated in phosphate-buffered saline (PBS)–0.002% saponin for 10 min at room temperature before continuing with a standard immunofluorescence assay as described previously (13). Saponin (0.002%) was included in all blocking, washing, and antibody incubation steps.

Immunoblotting. Immunoblotting was performed as described previously (41). Parasite lysates and excreted-secreted antigen (ESA) fractions were diluted in 95°C reducing sample buffer (sodium dodecyl sulfate [SDS] sample buffer with 2% β-mercaptoethanol), boiled for 3 min, vortexed, and pelleted before being loaded on 12.5% SDS–polyacrylamide gel electrophoresis (PAGE) gels.

Secretion assays. Assays examining constitutive or ethanol-induced microneme secretion from MIC5-complemented strains were performed as described previously (27). To examine the effect of ALLN and cytochalasin D on processing, parasites were incubated in 40 μg ml^{-1} ALLN (Roche), 1 μM cytochalasin D (Sigma), or 1% dimethyl sulfoxide (solvent control) for 10 min at room temperature before microneme release was stimulated with 1% ethanol at 37°C for 20 min. ESA preparations were collected as described previously (10).

Replication/growth assay. Replication assays were performed as described previously (27), with an additional time point of 17 h postinoculation. Numbers of vacuoles containing 1, 2, 4, 8, or 16 parasites were enumerated.

Gliding assay. Parasite gliding assays on plastic and glass slides were performed using a modified assay (42). Briefly, slides were coated overnight at 4°C with 50% FBS–PBS and rinsed with PBS. Parasites were washed extensively with Hanks balanced salt solution containing 0.001 M EGTA and 0.01 M HEPES at pH 7.2 and allowed to glide on slides for 23 min at 37°C. Slides were then fixed as described above and stained for SAG1. Parasite trail lengths were measured using RT-Spot advanced software by tracing the path of trails derived from parasites that remain bound to the substrate after staining.

Video microscopy and attachment and invasion assays. Video microscopy and laser scanning cytometer-based attachment and invasion assays were performed as previously described (34, 35), with the following changes: for the invasion assay, 1×10^6 parasites were plated per coverslip; for the invasion and attachment assays, parasites were passed through a 27-gauge needle prior to being plated on the host cell monolayer.

Virulence. The in vivo virulence of strains RH, Δ*MIC5*-1, Δ*MIC5*-2, Δ*MIC5*-1::*CAT-MIC5*, and Δ*MIC5*-2::*CAT-MIC5* was examined in 10-week-old Swiss-Webster mice (Charles River Laboratories) as follows. Between 2 and 5 tachyzoites (measured in parallel by plaque assay) of each strain were injected intraperitoneally into 7 mice per strain. Fulminant disease was then allowed to develop, and the percent survival per day was measured. Clearly sick mice that lived past 12 days postinoculation were humanely euthanized by asphyxiation with CO_2. Serum collected via the saphenous vein from mice showing no signs of toxoplasmosis by day 14 postinoculation was tested for immunoreactivity by enzyme-linked immunosorbent assay, using a standard protocol (24), and shown to be seronegative. Since these mice likely did not receive a viable inoculum, they were not included in the time-to-death data set.

DIGE. Concentrated ESA fractions were dialyzed against 3 mM Tris, pH 8.5, in Biospin 6 columns (Bio-Rad) according to the manufacturer's instructions. Protein concentrations in dialyzed samples were determined with the BCA assay (Pierce). Samples were then lyophilized to dryness and subjected to differential gel electrophoresis (DIGE) analysis as described previously (43).

CHO cell transfections. The open reading frames of MIC5 and MIC2 were cloned into the mammalian expression vector, pBUDCE4 (Invitrogen). Constructs were transfected into Chinese hamster ovary (CHO) cells using Lipofectamine 2000 reagent (Invitrogen) according to the manufacturer's directions. Briefly, 1.2×10^5 CHO cells were cultured per well in a 24-well plate in HFF

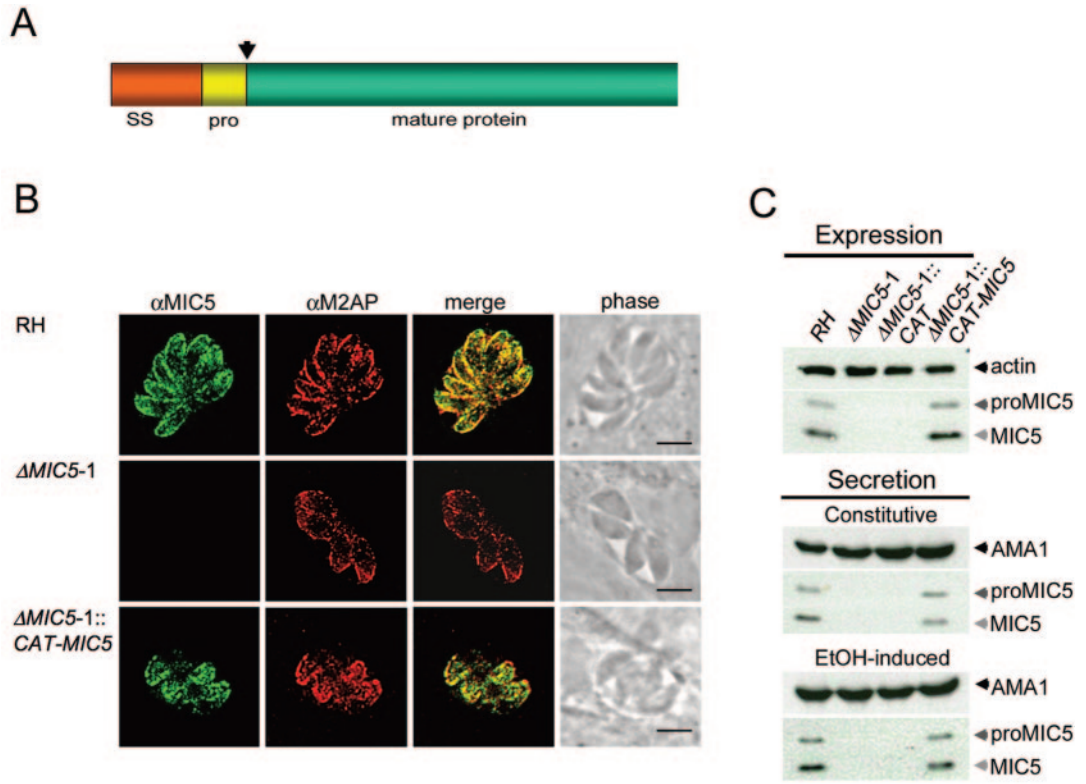

FIG. 1. MIC5 ablation and complementation. (A) MIC5 protein schematic, showing the 29-amino-acid (aa) signal sequence (SS), the 14-aa propeptide (pro) (arrow denotes cleavage site), and the 138-aa mature sequence. (B) Immunofluorescence analysis of intracellular parasites 24 h postinoculation. Monolayers were fully permeabilized with 0.2% Triton X-100 and stained with anti-MIC5 and anti-M2AP. Signals colocalize at the apical ends of RH and Δ*MIC5* complemented parasites (Δ*MIC5*-1::*CAT-MIC5*) arrayed outward in a rosette, whereas no MIC5-specific signal is observed in Δ*MIC5*-1. Bar, 5 μm. (C) Immunoblots of parasite lysates and constitutive and induced ESA fractions from RH, Δ*MIC5*-1, Δ*MIC5*-1::*CAT*, and Δ*MIC5*-1::*CAT-MIC5*.

medium without antibiotic, supplemented with 25% Ham's complete medium (Ham's medium [Biowhittaker] supplemented with 10% FBS) for 24 h. In duplicate, 2.4 μg of pBUDCE4 and equal molar amounts of pBUD-MIC5 and pBUD-MIC2, respectively, in 50 μl DMEM (no additions) were mixed with 50 μl of DMEM containing 2.8 μl Lipofectamine 2000 and incubated for 20 min at room temperature. DNA mixtures were then added directly to CHO cells, and transfection mixtures were incubated at 37°C. Eighteen hours later, one well of cells per construct was trypsinized, replated into one well of an eight-well chamber slide, and then incubated again. Twenty-four hours later, slides were subjected to saponin permeabilization and staining with mouse anti-H4 and MAb 6D10 anti-MIC2 in immunofluorescence assays as described above. CHO cells in the remaining transfection mixtures were separated into subcellular fractions as follows. Cell supernatants were collected, and cell monolayers were lysed by sonication. Sonicates were separated into cytoplasmic and membranous fractions by centrifugation. Secreted, cytoplasmic, and membrane-associated cell fractions were loaded in equal cell equivalents on SDS-PAGE gels and subjected to immunoblotting with mouse anti-H4 and MAb 6D10 anti-MIC2.

RESULTS

Genetic ablation and complementation of MIC5. MIC5 is a small MIC protein containing a secretory signal sequence followed by a 14-amino-acid propeptide that is removed during trafficking through the secretory system (8) (Fig. 1A). Although MIC5 contains a motif sequence similar to that seen in peptidyl-prolyl *cis-trans* isomerases (PPIases) of the parvulin family (8), recombinant MIC5 failed to show activity in either of two different types of PPIase assays (21, 28) using several parvulin substrate peptides (data not shown). It is unlikely that the lack of enzymatic activity is due to incorrect folding because recombinant MIC5 was expressed cytoplasmically in *Escherichia coli* at high levels, it remained fully soluble after purification and concentration to >5 mg/ml, and >95% was in a nonaggregated form based on dynamic light scattering analysis. Moreover, mature MIC5 polypeptide does not contain cysteine residues, thereby eliminating disulfide bond formation as a potential problem. Native MIC5 and recombinant MIC5 comigrate by one-dimensional SDS-PAGE (8), suggesting that neither has sizeable posttranslational modifications. Nonetheless, we cannot rule out the possibility that the recombinant protein lacks PPIase activity because of limitations of heterologous expression.

Sequence database searches suggest that MIC5-related proteins are expressed by other isosporoid coccidians including *Neospora caninum*, and *Sarcocystis neurona*, but not by other *Apicomplexa* such as *Eimeria*, *Cryptosporidium*, *Theileria*, or *Plasmodium*. Thus, MIC5 expression is limited to tissue cyst-forming coccidians.

We elected to use a reverse genetic approach to examine MIC5 function. To create an ablation construct for precise replacement of the *MIC5* open reading frame, we cloned *MIC5* 5′ (1.6 kb) and 3′ (2.5 kb) flanking sequences on either side of the selectable marker, HXGPRTase. The construct was electroporated into a parasite strain lacking expression of

HXGPRTase (Δ*HX*) (18), and parasite clones were selected with mycophenolic acid and xanthine (38). Multiple MIC5 knockout (Δ*MIC5*) clones from independent transfections were isolated. However, since these clones showed essentially the same phenotypes, the results from only one such clone, termed Δ*MIC5*-1, are presented. The absence of MIC5 expression in Δ*MIC5*-1 was verified by immunofluorescence staining (Fig. 1B, middle row) and immunoblotting (Fig. 1C).

To restore expression of MIC5, we transfected Δ*MIC5*-1 with a construct (p*MIC5*) containing the entire *MIC5* locus, including its endogenous promoter and polyadenylation signal. Selection was accomplished by cotransfection with a construct containing chloramphenicol acetyl transferase (p*CAT*), and a complemented clone, Δ*MIC5*-1::*CAT-MIC5*, was isolated. As a control for the presence of CAT, we also isolated a clone transfected with p*CAT* alone (Δ*MIC5*-1::*CAT*). All knockout and complement strains were subjected to Southern blotting with probes against *MIC5*, *HXGPRT*, and *CAT*, as appropriate, to validate the genetic manipulations (data not shown).

Localization and secretion of restored MIC5. Immunolocalization experiments for Δ*MIC5*-1::*CAT-MIC5* showed that it had restored apical MIC5 localization in a pattern similar to RH parasites, overlapping well with another micronemal protein, M2AP (Fig. 1B). Western blots of lysates showed a profile of MIC5 expression in RH and Δ*MIC5*-1::*CAT-MIC5* similar to that of two anti-MIC5-reacting bands observed corresponding to proMIC5 and mature MIC5, respectively. Mature MIC5 was approximately twice as abundant as proMIC5 (Fig. 1C, upper panel).

Parasites incubated at 37°C continually release both microneme and dense granule proteins at a basal level, whereas treatment with a low concentration of ethanol stimulates microneme secretion while slightly down-regulating dense granule exocytosis (10). To examine whether reexpression of MIC5 in Δ*MIC5*-1::*CAT-MIC5* supported normal secretion of MIC5, we subjected these clones to induced and constitutive microneme secretion assays. In both assays, Δ*MIC5*-1::*CAT-MIC5* secreted amounts of proMIC5 and mature MIC5 that were essentially indistinguishable from RH.

Δ*MIC5*-1 parasites exhibit normal growth, invasion, virulence, and localization of other micronemal proteins. As a first step toward evaluation of *MIC5* ablation and restoration, we examined the replication rates of RH, Δ*MIC5*-1, and Δ*MIC5*-1::*CAT-MIC5*. Essentially no difference in the percentages of vacuoles containing 1, 2, 4, and 8 parasites were observed among strains 18 h postinoculation (data not shown). At 27 h postinoculation, both Δ*MIC5*-1 and Δ*MIC5*-1::*CAT-MIC5* had slightly more vacuoles containing 8 parasites than RH. Since this small growth enhancement was not dependent on the presence or absence of MIC5, we conclude that MIC5 does not influence parasite replication.

RH, Δ*MIC5*-1, and Δ*MIC5*-1::*CAT-MIC5* parasites were also assessed for invasion efficiency using a conventional red-green invasion assay (15, 27), a laser-scanning cytometry invasion assay (35), and video microscopy. In all three assays, Δ*MIC5*-1 parasites invaded host cells at a level that was indistinguishable from RH (data not shown). Mice infected with Δ*MIC5*-1 also succumbed to the acute infection with the same time-to-death kinetics as mice infected with RH or Δ*MIC5*-1::*CAT-MIC5* (data not shown). The RH strain is highly lethal (100% lethal dose ≈ 1 tachyzoite), and this feature could mask a minor attenuation in virulence in Δ*MIC5*-1. Collectively, these results indicate that MIC5 is not required for *Toxoplasma* invasion or extreme virulence in mice.

Previous ablation of the transmembrane domain-containing protein, MIC6, caused soluble proteins MIC1 and MIC4 to be diverted to the dense granules and parasitophorous vacuole (40). Ablation of the soluble proteins MIC1 and M2AP also disrupted the trafficking of their respective associated proteins (27, 40). Thus, loss of expression of either soluble or membrane-associated proteins can disrupt trafficking of other micronemal proteins. We therefore stained intracellular Δ*MIC5*-1 parasites for microneme proteins, MIC1, MIC2, MIC3, MIC4, MIC6, MIC10, SUB1, AMA1, and M2AP. All of these proteins appeared apically localized in Δ*MIC5*-1 in a pattern indistinguishable from that of RH (data not shown). The localization of dense granule protein GRA4 and surface antigen protein SAG1 was also examined, and no difference between RH and Δ*MIC5* was observed.

DIGE analysis. As a way forward, we sought to view the potential influence of MIC5 on the wide repertoire of *Toxoplasma* secretory products using two-dimensional (2-D) DIGE. We isolated preparative scale ESA fractions from RH and Δ*MIC5*-1, labeled each protein population with a green (cy3) or red (cy5) dye, respectively, and combined them for separation on 2-D SDS-PAGE gels. Images were collected using filters specific for each fluorescent dye and then superimposed for analysis. Spots appearing green are more prevalent in RH (or missing in Δ*MIC5*-1 ESA), and red spots are more abundant in Δ*MIC5*-1 ESA. Yellow spots are equally represented in the two populations. The analysis was performed twice using independently isolated ESA preparations, and similar results were observed in both experiments.

Many differences in the two protein populations were observed, with several spots reduced or absent in Δ*MIC5*-1 ESA, including a prominent acidic ~20-kDa spot corresponding to MIC5 (Fig. 2A). Also, a small number of protein species appeared more prevalent in Δ*MIC5*-1 than in RH. Several of these spots were excised and identified by mass spectroscopy. Many of the changes appeared to involve proteolytic precursor/product relationships. For example, MIC2 is processed from an ~115-kDa cell-associated species to a 100-kDa ($MIC2^{100}$) secreted form, which undergoes N-terminal trimming by the protease MPP2 to a 95-kDa species ($MIC2^{95}$) (11). Both $MIC2^{100}$ and $MIC2^{95}$ are normally present in the ESA. DIGE analysis showed a decrease of $MIC2^{100}$ in Δ*MIC5*-1 and a slight increase in $MIC2^{95}$, especially in the basic region of the cluster. The 75-kDa cell-associated form of MIC4 is normally processed to a secreted form of 70 kDa ($MIC4^{70}$) and then further to fragments of 50 kDa ($MIC4^{50}$) and 20 kDa ($MIC4^{20}$). $MIC4^{70}$ was less abundant in Δ*MIC5*-1, whereas $MIC4^{50}$ was more abundant. The $MIC4^{20}$ C-terminal product seen in RH shifted in both size and charge, with Δ*MIC5*-1 producing a smaller and more basic product, $MIC4^{18}$. Since the cleavage of $MIC4^{70}$ to $MIC4^{50}$ and $MIC4^{20}$ is also mediated by MPP2 (5), these results indicate that the absence of MIC5 not only increases the abundance of MPP2 products but it can also affect the cleavage site specificity of the protease.

As shown by Miller and coworkers (33), SUB1 is processed both autocatalytically and by another protease to yield a series

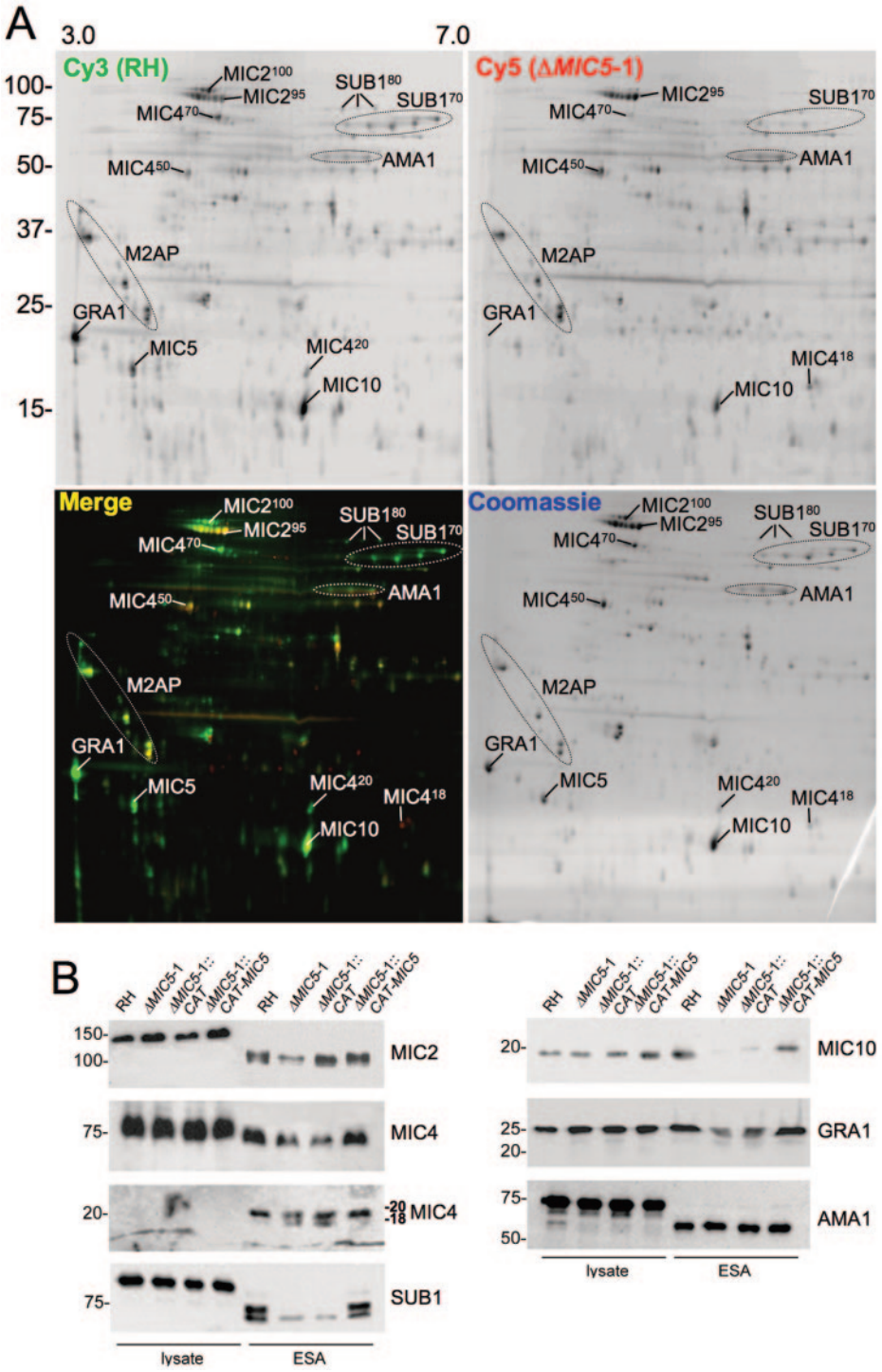

FIG. 2. Loss of MIC5 expression changes the ESA secretory profile. (A) Large-scale ESA fractions were isolated from Δ*MIC5*-1 and RH parasites, normalized as to protein content, and labeled with either cy5 (red) dye or cy3 (green) dye, respectively, before protein populations were combined and run together on 2-D SDS-PAGE. Following laser-scanning acquisition of the fluorescent images, the gel was stained with Coomassie blue dye to label all proteins. Top panels are images taken in single channels, whereas the bottom left panel is merged and the bottom right is the Coomassie-stained gel. Positions of various secreted proteins are indicated based on direct identification by mass spectroscopy or their migration relative to the previously described map of the *Toxoplasma* ESA proteome (44). (B) Western blots of parasite lysates and ESA fractions from RH, Δ*MIC5*-1, Δ*MIC5*-1::*CAT*, and Δ*MIC5*-1::*CAT-MIC5* strains probed with anti-SUB1, anti-MIC2, anti-MIC4, anti-MIC10, anti-GRA1, or anti-AMA1 antibodies.

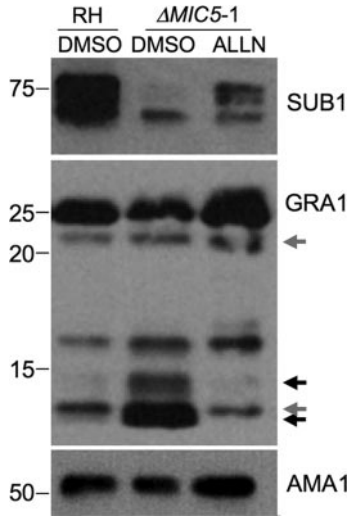

FIG. 3. MPP2-mediated proteolytic processing is responsible for the enhanced cleavage phenotype exhibited by Δ*MIC5*-1 parasites. Western blots of ESA fractions from RH or Δ*MIC5*-1 parasites treated with the protease inhibitor ALLN or dimethyl sulfoxide (DMSO, solvent control) and probed with anti-SUB1, anti-GRA1, or anti-AMA1. ALLN reverses the enhanced processing of SUB1 and GRA1. Gray and black arrows denote GRA1 fragments generated by ALLN-insensitive and -sensitive events, respectively. AMA1 is included as a loading control.

of species at ~80 kDa ($SUB1^{80}$) and ~70 kDa ($SUB1^{70}$). In Δ*MIC5*-1 ESA, $SUB1^{80}$ and the largest of the $SUB1^{70}$ species are much less abundant than in RH. Although we were unable to identify any smaller proteolytic products of SUB1 that would indicate proteolytic degradation, it is possible that these correspond to some of the red spots of insufficient abundance to excise for identification. MIC10, an 18-kDa microneme protein (25) that is not known to undergo processing, was also reduced in Δ*MIC5*-1 ESA. Similarly, GRA1, a 25-kDa unprocessed protein secreted from the dense granules, was substantially reduced in Δ*MIC5*-1. These results indicate that the effects of *MIC5* ablation were not restricted to proteins that are processed by MPP2 or derived from the micronemes. M2AP, which is extensively processed by MPP2 (and MPP3), was not dramatically affected by deletion of *MIC5*. Finally, many other ESA proteins were not affected by ablation of *MIC5*, including AMA1, a highly conserved microneme protein required for *Toxoplasma* invasion (34).

To confirm DIGE analysis findings, we performed Western blots of parasite cell lysates and analytical-scale ESA fractions (Fig. 2B). The results largely corroborate the DIGE findings. The N-terminally processed species of secreted MIC2 were difficult to resolve by one-dimensional SDS-PAGE, despite testing a variety of separation schemes and systems. A modest decrease in the largest species, $MIC2^{100}$, was seen (Fig. 2B; first panel, left) in most but not all experiments. More consistent were the changes seen for MIC4, including a reduction of $MIC4^{50}$ and $MIC4^{20}$ in Δ*MIC5*-1 relative to RH and the appearance of an extra 18-kDa species in Δ*MIC5*-1 and Δ*MIC5*-1::*CAT* ESAs (second and third panels, left). $SUB1^{80}$ and $SUB1^{70}$ are much less abundant in Δ*MIC5*-1 and Δ*MIC5*-1::*CAT* ESAs than RH (bottom panel, left). MIC10 and GRA1 are also reduced in Δ*MIC5*-1 and Δ*MIC5*-1::*CAT* ESAs (top and middle panels, right). The abundance of AMA1

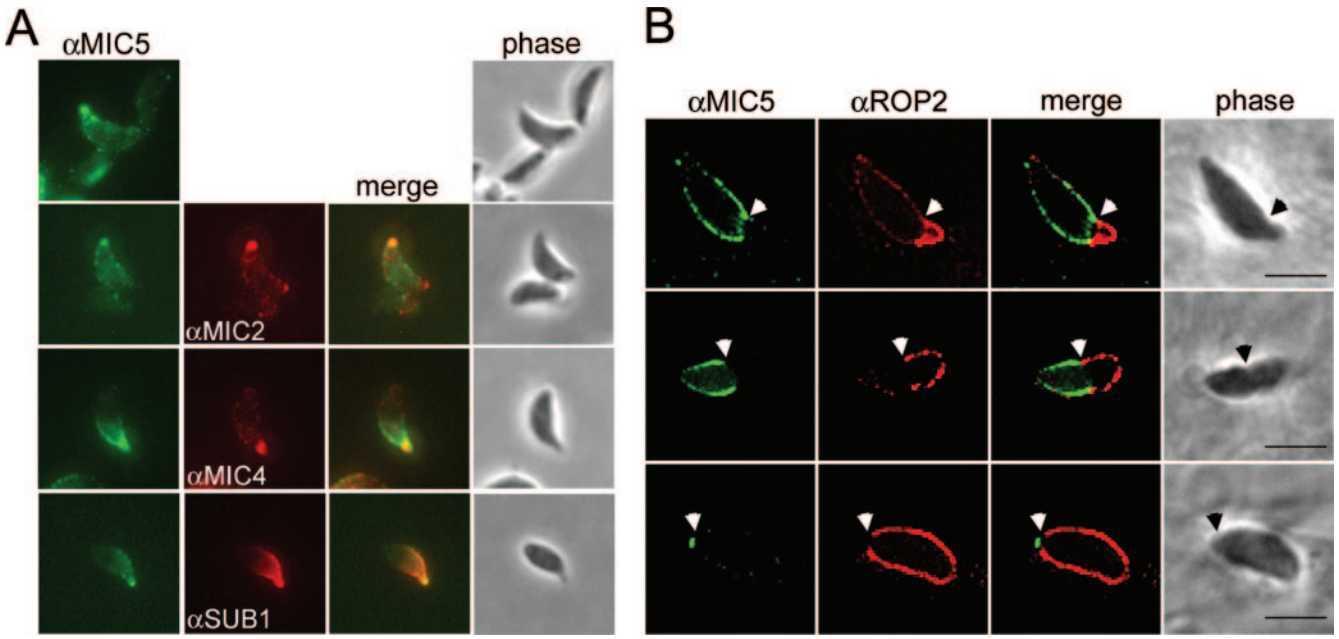

FIG. 4. MIC5 is exuded onto the parasite surface and labels a region near the moving junction during host cell invasion. (A) MIC5 partially colocalizes with MIC2, MIC4, and SUB1 on the surface of extracellular parasites stimulated to secrete microneme contents. Extracellular parasites were stimulated to release microneme contents, fixed, and subsequently labeled with anti-MIC5 (αMIC5), anti-MIC2 (αMIC2), and anti-SUB1 (αSUB1). (B) MIC5 labels a region near the moving junction between the parasite and host cell plasma membranes during invasion, treadmilling toward the posterior of the parasite as it penetrates into the PV. RH parasites added to HFF monolayers in a pulse were trapped in a partially invaded state and semipermeabilized to examine the contents of the PV without interference from signal within the parasite. Anti-ROP2 (αROP2) antibodies denote the PV. White arrows indicate the position of the moving junction. Bars, 5 μm.

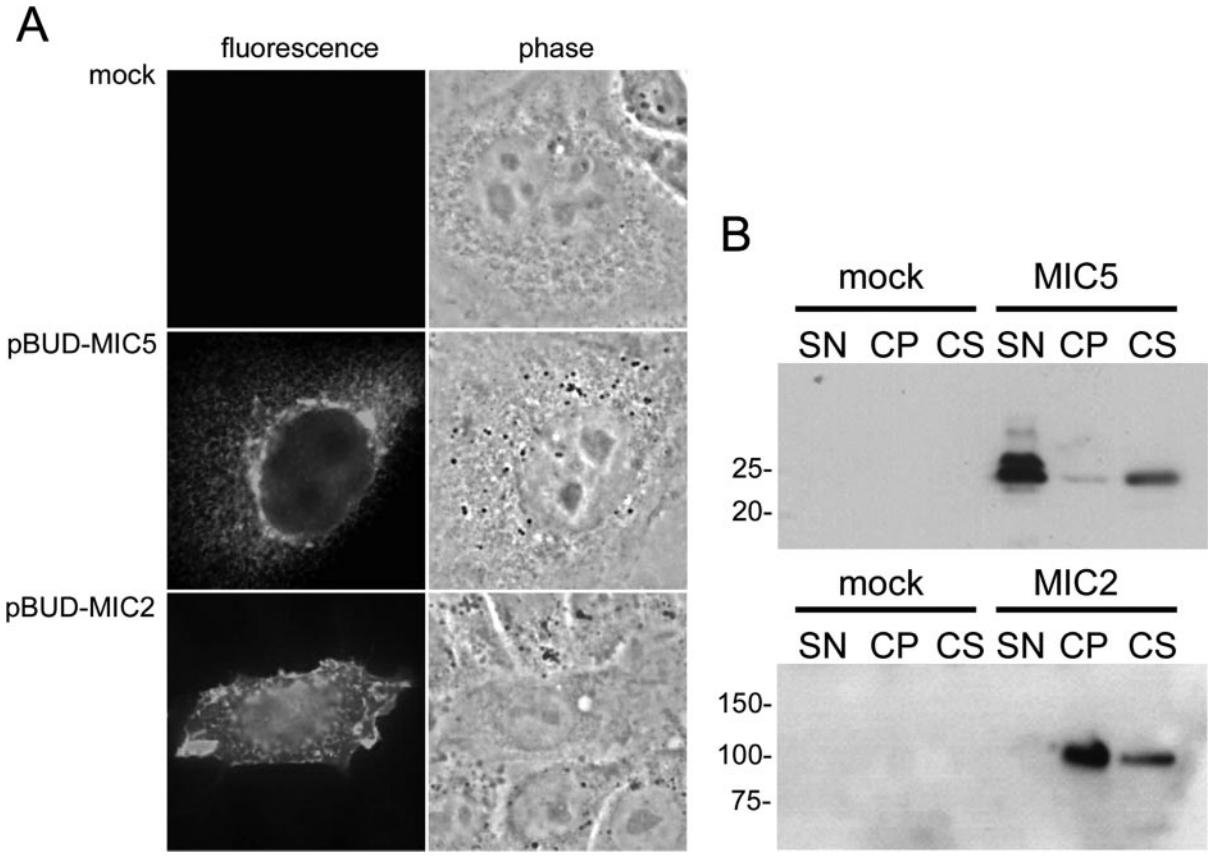

FIG. 5. MIC5 is not membrane associated when expressed in CHO cells. CHO cells transfected with constructs containing *MIC5* (pBUD-MIC5), *MIC2* (pBUD-MIC2), or empty vector (mock) were subjected to immunofluorescence assay (A) or separated into subcellular fractions (supernatant [SN], membrane [cell pellet {CP}], cytoplasmic [cell soluble {CS}]) and analyzed by immunoblotting (B). Whereas MIC2 is associated with the cell membrane by both microscopy (A) and subcellular fractionation (B), MIC5 is found almost exclusively in cytoplasmic vesicles via microscopy and in the cytoplasmic and supernatant fractions.

is similar among the strains (bottom panel, right), also corroborating the DIGE analysis. Analysis of the corresponding parasite lysates (first four lanes of each panel) revealed little variation, strongly suggesting that differences in ESA protein abundance are not because of effects on protein expression within the parasite.

Excess proteolysis in Δ*MIC5*-1 is partially reversed by treatment with ALLN. To further investigate proteolysis as a potential basis for the observed changes in ESA protein abundance, we examined the effects of treatment with ALLN, a tripeptide aldehyde inhibitor previously shown to block the activity of MPP2 (5, 11, 43). ALLN treatment of Δ*MIC5*-1 parasites restored the normal pattern of $SUB1^{80}$/$SUB1^{70}$ and GRA1 bands in ESA (Fig. 3). Based on these observations, we conclude that changes in the abundance and processing of ESA products are due, at least in part, to the action of the MPP2 protease.

MIC5 occupies the surface of secretion-activated and invading parasites. MPP2 activity was previously shown to be associated with the parasite surface, processing proteins only after they are secreted (11). Therefore, we next sought to determine whether MIC5 is also associated with the parasite surface where it could influence proteolysis. To activate microneme secretion, RH parasites were briefly stimulated with the calcium ionophore A23187, fixed, and stained for surface MIC5 and other microneme protein markers. Their protruding apex readily identified parasites that responded to the treatment, a consequence of calcium-activated extrusion of the cytoskeletal conoid. In contrast to solvent-treated parasites, which showed little or no MIC5 surface staining (data not shown), A23187-treated tachyzoites displayed MIC5 on the apical tip in the same vicinity as MIC2, MIC4, and SUB1 (Fig. 4A). This indicates that despite not having a membrane anchor itself, MIC5 remains associated with the parasite surface after secretion from the micronemes.

To examine MIC5's behavior during host cell invasion, we used a recently described pulse-invasion assay that promotes synchronous invasion (30). After fixation, the host cell plasma membrane and the parasitophorous vacuolar membrane (PVM) were selectively permeabilized, leaving the parasite plasma membrane intact to avoid detecting material still within micronemes (13). As previous studies have shown that ROP2 is secreted into the parasitophorous vacuole where it associates with the PVM (3), anti-ROP2 was used in conjunction with anti-MIC5 to delineate the nascent PVM. Consistent with the A23187 findings, MIC5 remained tethered to the parasite surface during invasion, and it was particularly abundant in the region near the moving junction, a tight apposition of the host

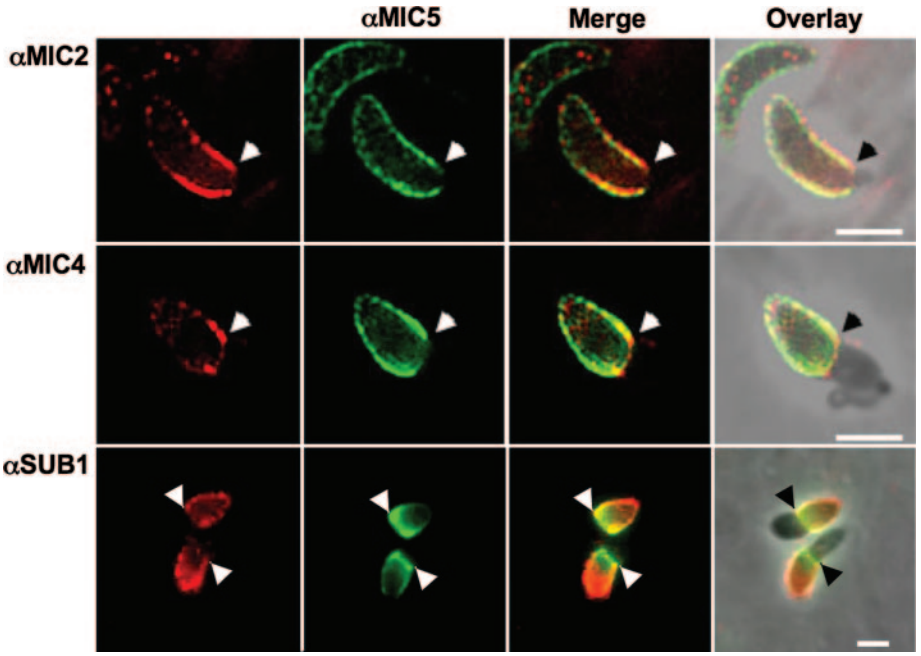

FIG. 6. MIC2, MIC4, and SUB1 label a region near the moving junction during invasion and partially colocalize with MIC5. Pulse-invaded parasites on HFF monolayers were semipermeabilized and stained with anti-MIC5 (αMIC5), anti-MIC2 (αMIC2), anti-MIC4 (αMIC4), and anti-SUB1 (αSUB1). MIC4 is almost exclusively positioned near the moving junction, whereas SUB1 labels the entire posterior of the parasite. MIC2 and MIC5 are intermediate in that they show some labeling of the parasite posterior but the majority of the signal is near the moving junction, denoted by arrows. A merge of two signals and a merge overlay onto the phase-contrast picture are shown. Bars, 5 μm.

and parasite plasma membranes that is often seen as a constriction at the "waist" of invading parasites (Fig. 4B, upper panels). MIC5 failed to cross the moving junction and instead was "capped" toward the posterior end in a phenomenon similar to that seen for other microneme proteins such as MIC2 (9) and MIC3 (23) (Fig. 4B, middle panels). Also like other microneme proteins, MIC5 appeared to be shed from the posterior surface during the final seconds of invasion (Fig. 4B, lower panels).

MIC5 does not have intrinsic membrane association properties. Analysis of the MIC5 protein sequence did not suggest the presence of a transmembrane domain or signal sequence for glycolipid or lipid addition. It does, however, remain possible that MIC5 can peripherally associate with membranes. To test this, we transiently expressed MIC5 in CHO cells and examined the expression pattern by immunofluorescence and immunoblotting (Fig. 5A and B). Although some MIC5 was observed within the cell in a perinuclear pattern (Fig. 5A, second panel), most of it was freely secreted into the culture supernatant (Fig. 5B). Also, the small amount of cell-associated MIC5 was largely soluble and not associated with the cell pellet. MIC2 was expressed as a positive control for membrane association, and as expected, it occupied the cell surface (Fig. 5A, third panel) and was primarily associated with the cell pellet (Fig. 5B). These findings indicate that MIC5 does not have intrinsic membrane binding properties and that its association with the parasite surface is likely indirect, possibly through an affiliation with another membrane-anchored microneme protein.

Proteins affected by targeted deletion of MIC5 partially colocalize with MIC5 during invasion. The behavior of MIC4, SUB1, and GRA1 during invasion has not been previously examined. To determine if these proteins decorate the parasite surface during entry, we dual stained invading RH parasites with anti-MIC5 and, respectively, anti-MIC2 (positive control), anti-MIC4, anti-SUB1, or anti-GRA1. Both MIC4 and SUB1 showed treadmilling behavior similar to MIC2, with MIC4 tightly localized near the moving junction and SUB1 often covering the entire extracellular portion of the parasite (Fig. 6). The extent of colocalization between proteins varied somewhat, but MIC5 was generally positioned intermediately between SUB1 and MIC4 relative to the moving junction. No surface staining with anti-GRA1 was observed (data not shown), which is consistent with earlier findings that GRA1 is not membrane associated (14). Collectively, these observations demonstrate that most, but not all, of the proteins affected by deletion of MIC5 occupy the parasite surface during invasion.

DISCUSSION

Proteolytic processing of micronemal proteins is commonly seen following secretion. Proteolytic shedding of TM MIC proteins, such as MIC2 and MIC6, is thought to break the connection between the parasite's motor system and host receptors, allowing the PV to close and completing the invasion process (6, 11). The role of proteolytic trimming events is less understood. Although surface trimming usually does not go to completion for parasites in the absence of host cells, complete trimming of the N-terminal extension from MIC2 was observed on parasites apically attached to human fibroblasts (11). Also, a recent study suggests that N-terminal trimming of MIC2 enhances its binding to intercellular adhesion molecule

1 (ICAM-1), which the parasite uses as a receptor for paracellular transmigration. When parasite lysates containing both full-length MIC2 and the N-terminally truncated product were incubated with ICAM-1-coated beads, only the truncated product was retained in the bound fraction. Binding was also abolished when lysates were prepared in the presence of chymostatin, which, like ALLN, inhibits MPP2 activity and prevents N-terminal trimming of MIC2. The investigators also showed that soluble ICAM-1 inhibits paracellular transmigration, presumably by preventing MIC2 from binding to cell surface-associated ICAM-1. Since *Toxoplasma* grows and eventually encysts in deep tissues, the ability to power through extracellular matrix and cellular junctions is likely crucial. Trimming of other MIC proteins may also regulate adhesive activity, especially since many of these proteins contain adhesive elements and bind host cells in vitro (5, 22, 23, 41).

Just how MIC5 regulates surface proteolytic activity is unclear. One possibility is that MIC5 regulates MPP2 directly through a physical interaction, limiting its activity to appropriate substrates and preventing proteolysis of inappropriate targets. The absence of MIC5 would result in unbridled MPP2 activity and enhanced proteolysis of both appropriate and inappropriate targets. This hypothesis seems unlikely, however, as processing of M2AP is largely unchanged in Δ*MIC5*-1, despite the obvious increase in processing of its partner, MIC2. It is difficult to envision the basis of such differential selectivity if MIC5 was acting directly as a protease inhibitor for MPP2. A second possibility is that MIC5 affects the susceptibility of substrates to proteolytic processing by influencing the conformation or organization of these substrates on the parasite surface. Indeed, MIC5 appears to be one of the most abundant secretory proteins, and therefore, its absence could indirectly influence the interactions of MIC proteins with each other or with other abundant surface components such as the SAGs. Preliminary analysis of size exclusion chromatography fractions of a parasite extract indicates that MIC5 exists in high-molecular-weight complexes, perhaps surrounding and organizing other secreted proteins on the cell surface. In this manner, MIC5 could influence substrate susceptibility to other proteases in addition to MPP2.

Determining how MIC5 is associated with the parasite surface may help distinguish among the above possibilities. Since MIC5 does not possess a membrane anchor and it fails to associate with the surface of CHO cells on its own, MIC5 probably interacts with a TM MIC protein for both trafficking to the micronemes and for retention on the parasite surface during invasion. However, it is unlikely that MIC5 interacts with MIC2, MIC6, or AMA1, since these proteins show normal trafficking to the micronemes in Δ*MIC5*-1, whereas in most cases examined so far, the absence of one component of a MIC protein complex impairs the trafficking of the remaining components (26, 40). Attempts to visualize proteins associated with MIC5 by immunoprecipitation using ^{35}S-labeled parasite extracts have failed to reveal evidence of a heterologous interaction, suggesting that the complex, if it exists, is fragile. Attempts to isolate binding partners by yeast two-hybrid screening (Michael Black, personal communication) were also unsuccessful. We are currently examining other putative MIC proteins identified in the ESA (44) for possible association with MIC5.

MIC10 and GRA1 are normally secreted intact into the ESA, suggesting that proteolysis of these proteins is not an enhancement of a normal process, but an aberrant side effect. As no MIC10 fragments were found in Δ*MIC5* ESA, we cannot determine whether MIC10 is simply degraded to small fragments not retained on gels, or is not secreted due to loss of a separate function of MIC5 that is unrelated to proteolysis. Neither MIC10 nor GRA1 have been shown to associate with the parasite surface, suggesting that they may be degraded after secretion as soluble products into the ESA. In this case, the observations would be more consistent with an elevation in proteolytic activity in the ESA rather than an effect on susceptibility of the substrate to proteolysis. Two proteases have been reported to be present in the ESA, SUB1 and a putative metalloproteinase encoded by the predicted gene TwinScan 4000 (Ts4000) (44). SUB1 is a glycosylphosphatidylinositol-anchored serine protease of the subtilase family, whereas TS4000 is a member of the insulinase family. The substrate specificity of either enzyme has not been determined. Additional studies will be required to determine whether one or both of these enzymes are directly or indirectly regulated by MIC5.

The lack of an effect on parasite invasion and virulence is perhaps surprising, given the number of changes observed in the proteolysis of secreted proteins, including several adhesins. However, ablation studies of other secreted proteins have indicated that redundancy in adhesive mechanisms exists in *Toxoplasma*, possibly accounting for its wide host range. MIC5's effect on processing might result in the impairment of invasion of a subset of cells only encountered during in vivo infection. We did not explore the effect of ablation of MIC5 on cyst formation and the establishment of chronic infection, as the strain we used does not form cysts readily. Perhaps if cyst-forming strains of *Toxoplasma* become more amenable to genetic manipulation, MIC5's role during chronic infection can be elucidated.

ACKNOWLEDGMENTS

We are especially indebted to Thilo Kamphausen and Gunter Fischer for testing recombinant MIC5 for PPIase activity. We also thank Gale Sherman and Claudia Bordon for technical help and Kami Kim, Theresa Shapiro, Paul Englund, David Sullivan, and Sharon Krag for their invaluable suggestions for this study.

This work was supported by funds from the NIH (AI53797 to V.B.C.; AI63276 to G.E.W.), the Forschungsforderung University of Dusseldorf (K.D.Z.A.), and the Deutsche Forschungsgemeinschaft (SPP 1130 to W.D.).

REFERENCES

1. **Achbarou, A., O. Mercereau-Puijalon, J. M. Autherman, B. Fortier, D. Camus, and J.-F. Dubremetz.** 1991. Characterization of microneme proteins of *Toxoplasma gondii*. Mol. Biochem. Parasitol. **47:**223–234.
2. **Barta, J. R., D. S. Martin, R. A. Carreno, M. E. Siddall, H. Profous-Juchelkat, M. Hozza, M. A. Powles, and C. Sundermann.** 2001. Molecular phylogeny of the other tissue coccidia: *Lankesterella* and *Caryospora*. J. Parasitol. **87:**121–127.
3. **Beckers, C. J. M., J.-F. Dubremetz, O. Mercereau-Puijalon, and K. A. Joiner.** 1994. The *Toxoplasma gondii* rhoptry protein ROP2 is inserted into the parasitophorous vacuole membrane, surrounding the intracellular parasite, and is exposed to the host cell cytoplasm. J. Cell Biol. **127:**947–961.
4. **Blackman, M. J., H. Fujioka, W. H. Stafford, M. Sajid, B. Clough, S. L. Fleck, M. Aikawa, M. Grainger, and F. Hackett.** 1998. A subtilisin-like protein in secretory organelles of *Plasmodium falciparum* merozoites. J. Biol. Chem. **273:**23398–23409.
5. **Brecht, S., V. B. Carruthers, D. J. Ferguson, O. K. Giddings, G. Wang, U. Jaekle, J. M. Harper, L. D. Sibley, and D. Soldati.** 2001. The *Toxoplasma* micronemal protein MIC4 is an adhesin composed of six conserved apple domains. J. Biol. Chem. **276:**4119–4127.

6. **Brossier, F., T. J. Jewett, J. L. Lovett, and L. D. Sibley.** 2003. C-terminal processing of the *Toxoplasma* protein MIC2 is essential for invasion into host cells. J. Biol. Chem. **278:**6229–6234.
7. **Brossier, F., T. J. Jewett, L. D. Sibley, and S. Urban.** 2005. A spatially localized rhomboid protease cleaves cell surface adhesins essential for invasion by *Toxoplasma*. Proc. Natl. Acad. Sci. USA **102:**4146–4151.
8. **Brydges, S. D., G. D. Sherman, S. Nockemann, A. Loyens, W. Daubener, J. F. Dubremetz, and V. B. Carruthers.** 2000. Molecular characterization of TgMIC5, a proteolytically processed antigen secreted from the micronemes of *Toxoplasma gondii*. Mol. Biochem. Parasitol. **111:**51–66.
9. **Carruthers, V. B., O. K. Giddings, and L. D. Sibley.** 1999. Secretion of micronemal proteins is associated with *Toxoplasma* invasion of host cells. Cell. Microbiol. **1:**225–235.
10. **Carruthers, V. B., S. N. J. Moreno, and L. D. Sibley.** 1999. Ethanol and acetaldehyde elevate intracellular calcium and stimulate microneme discharge in *Toxoplasma gondii*. Biochem. J. **342:**379–386.
11. **Carruthers, V. B., G. D. Sherman, and L. D. Sibley.** 2000. The *Toxoplasma* adhesive protein MIC2 is proteolytically processed at multiple sites by two parasite-derived proteases. J. Biol. Chem. **275:**14346–14353.
12. **Carruthers, V. B., and L. D. Sibley.** 1999. Mobilization of intracellular calcium stimulates microneme discharge in *Toxoplasma gondii*. Mol. Microbiol. **31:**421–428.
13. **Carruthers, V. B., and L. D. Sibley.** 1997. Sequential protein secretion from three distinct organelles of *Toxoplasma gondii* accompanies invasion of human fibroblasts. Eur. J. Cell Biol. **73:**114–123.
14. **Cesbron-Delauw, M. F., B. Guy, R. J. Pierce, G. Lenzen, J. Y. Cesbron, H. Charif, P. Lepage, F. Darcy, J. P. Lecocq, and A. Capron.** 1989. Molecular characterization of a 23-kilodalton major antigen secreted by *Toxoplasma gondii*. Proc. Natl. Acad. Sci. USA **86:**7537–7541.
15. **Dobrowolski, J. M., V. B. Carruthers, and L. D. Sibley.** 1997. Participation of myosin in gliding motility and host cell invasion by *Toxoplasma gondii*. Mol. Microbiol. **26:**163–173.
16. **Dobrowolski, J. M., I. R. Niesman, and L. D. Sibley.** 1997. Actin in the parasite *Toxoplasma gondii* is encoded by a single copy gene, *ACT1* and exists primarily in a globular form. Cell Motil. Cytoskeleton **37:**253–262.
17. **Donahue, C. G., V. B. Carruthers, S. D. Gilk, and G. E. Ward.** 2000. The *Toxoplasma* homolog of *Plasmodium* apical membrane antigen-1 (AMA-1) is a microneme protein secreted in response to elevated intracellular calcium levels. Mol. Biochem. Parasitol. **111:**15–30.
18. **Donald, R. G., D. Carter, B. Ullman, and D. S. Roos.** 1996. Insertional tagging, cloning, and expression of the *Toxoplasma gondii* hypoxanthine-xanthine-guanine phosphoribosyltransferase gene. Use as a selectable marker for stable transformation. J. Biol. Chem. **271:**14010–14019.
19. **Dowse, T. J., J. C. Pascall, K. D. Brown, and D. Soldati.** 2005. Apicomplexan rhomboids have a potential role in microneme protein cleavage during host cell invasion. Int. J. Parasitol. **35:**747–756.
20. **Endo, T., H. Tokuda, K. Yagita, and T. Koyama.** 1987. Effects of extracellular potassium on acid release and motility initiation in *Toxoplasma gondii*. J. Protozool. **34:**291–295.
21. **Fischer, G., H. Bang, E. Berger, and A. Schellenberger.** 1984. Conformational specificity of chymotrypsin toward proline-containing substrates. Biochim. Biophys. Acta **791:**87–97.
22. **Fourmaux, M. N., A. Achbarou, O. Mercereau-Puijalon, C. Biderre, I. Briche, A. Loyens, C. Odberg-Ferragut, D. Camus, and J.-F. Dubremetz.** 1996. The MIC1 microneme protein of *Toxoplasma gondii* contains a duplicate receptor-like domain and binds to host cell surface. Mol. Biochem. Parasitol. **83:**201–210.
23. **Garcia-Réguet, N., M. Lebrun, M.-N. Fourmaux, O. Mercereau-Puijalon, T. Mann, C. J. M. Beckers, B. Samyn, J. Van Beeumen, D. Bout, and J.-F. Dubremetz.** 2000. The microneme protein MIC3 of *Toxoplasma gondii* is a secretory adhesin that binds to both the surface of the host cells and the surface of the parasite. Cell. Microbiol. **2:**353–364.
24. **Harlow, E., and D. Lane.** 1988. Antibodies: a laboratory manual. Cold Spring Harbor Laboratory, Cold Spring Harbor, N.Y.
25. **Hoff, E. F., S. H. Cook, G. D. Sherman, J. M. Harper, D. J. Ferguson, J. F. Dubremetz, and V. B. Carruthers.** 2001. *Toxoplasma gondii*: molecular cloning and characterization of a novel 18-kDa secretory antigen, TgMIC10. Exp. Parasitol. **97:**77–88.
26. **Huynh, M. H., C. Opitz, L. Y. Kwok, F. M. Tomley, V. B. Carruthers, and D. Soldati.** 2004. Trans-genera reconstitution and complementation of an adhesion complex in *Toxoplasma gondii*. Cell. Microbiol. **6:**771–782.
27. **Huynh, M. H., K. E. Rabenau, J. M. Harper, W. L. Beatty, L. D. Sibley, and V. B. Carruthers.** 2003. Rapid invasion of host cells by *Toxoplasma* requires secretion of the MIC2-M2AP adhesive protein complex. EMBO J. **22:**2082–2090.
28. **Janowski, B., S. Wollner, M. Schutkowski, and G. Fischer.** 1997. A protease-free assay for peptidyl prolyl cis/trans isomerases using standard peptide substrates. Anal. Biochem. **252:**299–307.
29. **Johnson, A. M., and S. Illana.** 1991. Cloning of *Toxoplasma gondii* gene fragments encoding diagnostic antigens. Gene **99:**127–132.
30. **Kafsack, B. F. C., C. J. M. Beckers, and V. B. Carruthers.** 2004. Synchronous invasion of host cells by *Toxoplasma gondii*. Mol. Biochem. Parasitol. **136:**309–311.
31. **Labruyere, E., M. Lingnau, C. Mercier, and L. D. Sibley.** 1999. Differential membrane targeting of the secretory proteins GRA4 and GRA6 within the parasitophorous vacuole formed by *Toxoplasma gondii*. Mol. Biochem. Parasitol. **102:**311–324.
32. **Meissner, M., M. Reiss, N. Viebig, V. Carruthers, C. Toursel, S. Tomavo, J. Ajioka, and D. Soldati.** 2002. A family of transmembrane microneme proteins of *Toxoplasma gondii* contain EGF-like domains and function as escorters. J. Cell Sci. **115:**563–574.
33. **Miller, S. A., E. M. Binder, M. J. Blackman, V. B. Carruthers, and K. Kim.** 2001. A conserved subtilisin-like protein TgSUB1 in microneme organelles of *Toxoplasma gondii*. J. Biol. Chem. **276:**45341–45348.
34. **Mital, J., M. Meissner, D. Soldati, and G. E. Ward.** 2005. Conditional expression of *Toxoplasma gondii* apical membrane antigen-1 (TgAMA1) demonstrates that TgAMA1 plays a critical role in host cell invasion. Mol. Biol. Cell **16:**4341–4349.
35. **Mital, J., J. Schwarz, D. J. Taatjes, and G. E. Ward.** 2006. Laser scanning cytometer-based assays for measuring host cell attachment and invasion by the human pathogen *Toxoplasma gondii*. Cytometry A **69:**13–19.
36. **Opitz, C., M. Di Cristina, M. Reiss, T. Ruppert, A. Crisanti, and D. Soldati.** 2002. Intramembrane cleavage of microneme proteins at the surface of the apicomplexan parasite *Toxoplasma gondii*. EMBO J. **21:**1577–1585.
37. **Opitz, C., and D. Soldati.** 2002. 'The glideosome': a dynamic complex powering gliding motion and host cell invasion by *Toxoplasma gondii*. Mol. Microbiol. **45:**597–604.
38. **Pfefferkorn, E. R., and S. E. Borotz.** 1994. *Toxoplasma gondii*: characterization of a mutant resistant to 6-thioxanthine. Exp. Parasitol. **79:**374–382.
39. **Rabenau, K. E., A. Sohrabi, A. Tripathy, C. Reitter, J. W. Ajioka, F. M. Tomley, and V. B. Carruthers.** 2001. TgM2AP participates in *Toxoplasma gondii* invasion of host cells and is tightly associated with the adhesive protein TgMIC2. Mol. Microbiol. **41:**537–547.
40. **Reiss, M., N. Viebig, S. Brecht, M. N. Fourmaux, M. Soete, M. Di Cristina, J. F. Dubremetz, and D. Soldati.** 2001. Identification and characterization of an escorter for two secretory adhesins in *Toxoplasma gondii*. J. Cell Biol. **152:**563–578.
41. **Wan, K. L., V. B. Carruthers, L. D. Sibley, and J. W. Ajioka.** 1997. Molecular characterization of an expressed sequence tag locus of *Toxoplasma gondii* encoding the micronemal protein MIC2. Mol. Biochem. Parasitol. **84:**203–214.
42. **Wetzel, D. M., S. Hakansson, K. Hu, D. Roos, and L. D. Sibley.** 2003. Actin filament polymerization regulates gliding motility by apicomplexan parasites. Mol. Biol. Cell **14:**396–406.
43. **Zhou, X. W., M. J. Blackman, S. A. Howell, and V. B. Carruthers.** 2004. Proteomic analysis of cleavage events reveals a dynamic two-step mechanism for proteolysis of a key parasite adhesive complex. Mol. Cell. Proteomics **3:**565–576.
44. **Zhou, X. W., B. F. Kafsack, R. N. Cole, P. Beckett, R. F. Shen, and V. B. Carruthers.** 2005. The opportunistic pathogen *Toxoplasma gondii* deploys a diverse legion of invasion and survival proteins. J. Biol. Chem. **280:**34233–34244.